Reduced Dimensionality in Triple-Resonance NMR Experiments

T. Szyperski, G. Wider, J. H. Bushweller, and K. Wüthrich*

Institut für Molekularbiologie und Biophysik
Eidgenössische Technische Hochschule-Hönggerberg
CH-8093 Zürich, Switzerland

Received April 30, 1993

As an alternative to the conventional assignment of protein NMR[1] spectra by observation of sequential NOEs[2] in homonuclear 2D [^{1}H,^{1}H]-NOESY or 3D and 4D heteronuclear-resolved [^{1}H,^{1}H]-NOESY spectra, 3D and 4D triple-resonance experiments have been proposed for establishing intra- and interresidual connectivities via heteronuclear scalar couplings.[3-12] 4D experiments of this type are conceptually particularly attractive, since only a single experiment is needed for intraresidual correlation of the four backbone spins $^1H^N$, ^{15}N, $^{13}C^\alpha$, and $^1H^\alpha$, and suitable combinations of two 4D experiments can provide sequential assignments.[11,13] However, because of the short T_2 relaxation times of $^{13}C^\alpha$ in bigger molecules, the use of 4D triple resonance experiments[6,9,11] is in practice limited to proteins with molecular weights below approximately 15 000,[6] where such spectra are only sparsely populated with cross peaks and hence dispersion in four dimensions is not really needed. Therefore, the development of variant triple-resonance experiments that provide the same connectivity information in spectra with reduced dimensionality is attractive, since larger values of t_{max} can then be chosen for the indirect dimensions, more extensive phase cycling is feasible within the same accumulation time, and the smaller data sets facilitate data handling and processing. Recently, we presented an experimental scheme that used $^{13}C^\alpha$–^{15}N heteronuclear two-spin coherence to obtain spectra with reduced dimensionality.[14] The present communication introduces a more general projection technique which does not require the generation of two-spin coherence and can readily be used with all presently available triple-resonance NMR schemes.

To demonstrate the utility of the proposed projection technique, we recorded a 3D HA CA N HN experiment (the underlined letters indicate that the ^{15}N and $^{13}C^\alpha$ chemical shifts evolve simultaneously as single-quantum coherences) (Figure 1), which was derived from the 4D pulse sequence developed by Boucher *et al.*,[11] except that in view of the long T_2 relaxation time for the carbonyl carbon, ^{15}N and $^{13}C^\alpha$ are decoupled from $^{13}C{=}O$ with selective 180° pulses on $^{13}C{=}O$ instead of a WALTZ-16 sequence (Figure 2). Following Boucher *et al.*,[11] the transfer

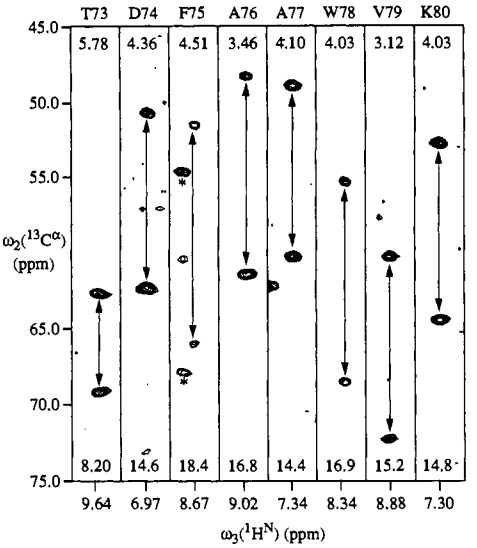

Figure 1. Contour plots of ($\omega_1(^{13}C^\alpha) - \omega_3(^1H^N)$)-strips from a 3D HA CA N HN spectrum obtained with a 2.5 mM sample of the uniformly ^{13}C- and ^{15}N-labeled mixed disulfide of *E. coli* glutaredoxin-(C14S) with glutathione[17] in 90% H_2O/10% D_2O, 100 mM potassium phosphate, pH 6.5, at T = 20 °C. A Bruker AMX 600 spectrometer equipped with four channels was used. 24 (t_1) * 98 (t_2) * 512 (t_3) complex points were accumulated, with $t_{1max}(^1H^\alpha)$ = 16.8 ms, $t_{2max}(^{15}N,^{13}C^\alpha)$ = 11.2 ms, and $t_{3max}(^1H^N)$ = 65.5 ms. 32 scans per increment were acquired, resulting in a total measuring time of 3.5 days. The carrier frequencies of the ^{15}N and $^{13}C^\alpha$ pulses were set to 105.1 and 56 ppm, respectively. Phase-sensitive detection was achieved using States-TPPI[16] in t_1 and t_2, so that the peak positions along ω_2 are at $\Omega(^{13}C^\alpha) \pm \Omega(^{15}N)$. In addition to the purge pulse (Figure 2), the water signal was further reduced with the convolution method of Marion *et al.*[21] The digital resolution after zero-filling was 22 Hz along ω_1, 34 Hz along ω_2, and 7.6 Hz along ω_3. Prior to Fourier transformation, the data were multipled with a sine bell window shifted by 45° in t_1, and a cosine window in t_2 and t_3.[22] No linear prediction or maximum entropy processing was applied. The spectrum was processed using the program PROSA.[23] The strips were taken at the $^1H^\alpha$ chemical shifts of the residues 73–80. The sequence-specific assignments are indicated at the top of each strip by the one-letter amino acid symbol and the sequence position, the $^1H^\alpha$ chemical shift along ω_1 is given in ppm below the resonance assignment, the $^1H^N$ chemical shifts around which the strips are centered along ω_3 are indicated in ppm below each strip, and the axes along ω_2 gives the chemical shift of the $^{13}C^\alpha$ nuclei. The chemical shifts of the ^{15}N nuclei relative to the ^{15}N carrier frequency (105.1 ppm), which were extracted from the in-phase splittings indicated by the arrows, are given at the bottom of each strip. Additional peaks in the strip of F75 (marked with an asterisk) belong to V64.

amplitude that produces the peak patterns observed in 3D HA CA N HN spectra was evaluated using the product-operator formalism.[15] Thereby, only terms resulting in observable magnetization during the detection period were retained, relaxation terms and constant multiplicative factors were omitted, and interresidue transfer of magnetization via the two-bond $^{13}C_i^\alpha - {}^{15}N_{i+1}$ coupling was neglected. Provided that $2\tau_1 = \tau_2 = {}^1/_2[^1J(^{13}C^\alpha, {}^1H^\alpha)]$ and $\tau_5 = 2\tau_6 = {}^1/_2[^1J(^{15}N, {}^1H^N)]$ (Figure 2), the observable magnetization at the beginning of the acquistion is given by (1),

$$\sigma(t_3 = 0) = I_x^N \cos[\Omega(^1H^\alpha)t_1] \cos[\Omega(^{13}C^\alpha)t_2] \cos[\Omega(^{15}N)t_2] \quad (1)$$

where I^N is the spin operator for the amide proton and $\Omega(X)$ denotes the chemical shift of spin X. As described previously in the context of two-spin coherence spectroscopy,[14] $\sigma(t_3 = 0)$ contains the sum and the difference of the chemical shifts of $^{13}C^\alpha$ and ^{15}N, which can be detected in a phase-sensitive manner by

(1) Abbreviations used: NMR, nuclear magnetic resonance; 2D, two-dimensional; 3D, three-dimensional; 4D, four-dimensional; NOE, nuclear Overhauser effect; NOESY, 2D NOE spectroscopy; TPPI, time-proportional phase incrementation; glutaredoxin(C14S), mutant glutaredoxin with Cys 14 replaced by Ser.

(2) Wüthrich, K. *NMR of Proteins and Nucleic Acids*; Wiley: New York, 1986.
(3) Ikura, M.; Kay, L. E.; Bax, A. *Biochemistry* **1990**, *29*, 4659–4667.
(4) Kay, L. E.; Ikura, M.; Tschudin, R.; Bax, A. *J. Magn. Reson.* **1990**, *89*, 496–514.
(5) Kay, L. E.; Ikura, M.; Bax, A. *J. Magn. Reson.* **1991**, *91*, 84–92.
(6) Kay, L. E.; Wittekind, M.; McCoy, M. A.; Friedrichs, M. S.; Mueller, L. *J. Magn. Reson.* **1992**, *98*, 443–450.
(7) Bax, A.; Ikura, M. *J. Biomol. NMR* **1991**, *1*, 99–104.
(8) Powers, R.; Gronenborn, A. M.; Clore, G. M.; Bax, A. *J. Magn. Reson.* **1991**, *94*, 209–213.
(9) Boucher, W.; Laue, E. D. *J. Am. Chem. Soc.* **1992**, *114*, 2262–2264.
(10) Clubb, R. T.; Thanabal, V.; Wagner, G. *J. Biomol. NMR* **1992**, *2*, 203–210.
(11) Boucher, W.; Laue, E. D.; Campbell-Burk, S. L.; Domaille, P. J. *J. Biomol. NMR* **1992**, *2*, 631–637.
(12) Olejniczak, E. T.; Xu, R. X.; Petros, A. M.; Fesik, S. W. *J. Magn. Reson.* **1992**, *100*, 444–450.
(13) Bax, A.; Grzesiek, S. *Acc. Chem. Res.* **1993**, *26*, 131–138.
(14) Szyperski, T.; Wider, G.; Bushweller, J. H.; Wüthrich, K. *J. Biomol. NMR* **1993**, *3*, 127–132.
(15) Sørensen, O. W.; Eich, G. W.; Levitt, M. H.; Bodenhausen, G.; Ernst, R. R. *Prog. Nucl. Magn. Reson. Spectrosc.* **1983**, *16*, 163–192.

0002-7863/93/1515-9307$04.00/0

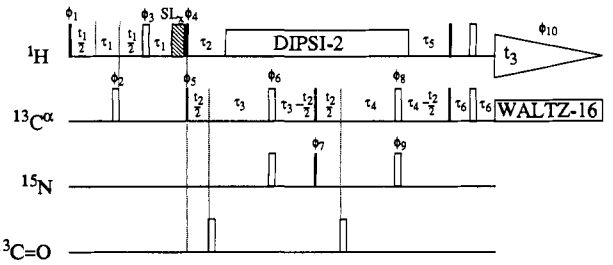

Figure 2. Experimental scheme for the 3D HA CA N HN experiment derived from the 4D HA CA N HN experiment of Boucher *et al.*[11] 90° and 180° pulses are indicated by thin and thick vertical bars, respectively, and the phases are indicated above the pulses. Where no radio frequency phase is marked, the pulse is applied along x. A spin-lock pulse, SL$_x$, of 2-ms duration is used to suppress the water signal.[24] The delays were set to the following values: τ_1 = 1.5 ms, $\tau_2 = {}^1/_2[{}^1J({}^1H^\alpha,{}^{13}C^\alpha)]$ = 3.4 ms, τ_3 = 12.564 ms, τ_4 = 11.664 ms, $\tau_5 = {}^1/_2[{}^1J({}^1H^N,{}^{15}N)]$ = 5.4 ms, τ_6 = 2.5 ms. A DIPSI-2[25] sequence is used to decouple ^{1}H during the heteronuclear magnetization transfer from $^{13}C^\alpha$ to ^{15}N, and a WALTZ-16 decoupling sequence is used during proton detection.[26] Phase cycling: $\phi_1 = 16(x)$; $\phi_2 = 8\{2x, 2(-x)\}$; $\phi_3 = 16(x, -x)$; $\phi_4 = 8\{2y, 2(-y)\}$; $\phi_5 = 2\{8(x), 8(-x)\}$; $\phi_6 = 4\{4(x), 4(y), 4(-x), 4(-y)\}$; $\phi_7 = \phi_8 = 16(x, -x)$; $\phi_9 = 2\{16(x), 16(-x)\}$; ϕ_{10} (receiver) = $\{x,-x,-x,x, 2(-x,x,x,-x), x,-x,-x,x\}$. Quadrature detection in t_1 and t_2 is accomplished by altering the phases ϕ_1 and ϕ_5, respectively, according to States-TPPI.[16]

applying the States-TPPI method[16] either to $^{13}C^\alpha$ or to ^{15}N. In the experiment of Figure 1, States-TPPI[16] was applied to $^{13}C^\alpha$, yielding resonances at $\Omega(^{13}C^\alpha) \pm \Omega(^{15}N)$ along the frequency axis ω_2 in the 3D HA CA N HN spectrum. Since the ^{15}N chemical shift is extracted from the difference between $\Omega(^{13}C^\alpha) - \Omega(^{15}N)$ and $\Omega(^{13}C^\alpha) + \Omega(^{15}N)$, the ^{15}N carrier must be at the edge of the ^{15}N spectral range to obtain unambiguous ^{15}N assignments. As the sweep width for ^{15}N (<2000 Hz at 14.1 T) is significantly smaller than that for $^{13}C^\alpha$ (~4500 Hz at 14.1 T), the thus required sweep width along ω_2 is only about one-third larger than in a corresponding 4D experiment. (This increase in sweep width could be circumvented if the in-phase splitting due to $\Omega(^{15}N)$ were scaled down using a smaller increment for ^{15}N than for $^{13}C^\alpha$, which would, however, also reduce $t_{max}(^{15}N)$).

Figure 1 shows contour plots of $(\omega_2(^{13}C^\alpha),\omega_3(^1H^N))$-strips at given $^1H^\alpha$ chemical shifts from a 3D HA CA N HN spectrum of a 2.5 mM solution of the ^{13}C,^{15}N-doubly-labeled mixed disulfide between glutaredoxin(C14S) and glutathione,[17] which has a molecular weight of 11 kDa. Each pair of peaks encodes the four backbone resonance frequencies of $^1H^\alpha$, $^1H^N$, $^{13}C^\alpha$, and ^{15}N for a particular residue: the $^1H^\alpha$ and $^1H^N$ chemical shifts were directly obtained from the positions of the peak pairs in the 3D spectrum, the center of the peak pair yields the $^{13}C^\alpha$ chemical shift, and the separation of the two peaks is equal to twice the offset of the amide nitrogen resonance from the ^{15}N carrier frequency. In the presently studied molecule, all backbone resonances could thus be assigned, with the sole exceptions of the six Gly and the three Pro, for obvious reasons, and Gln 66, which is not observable due to exchange broadening.[18] This result is equivalent to what one could expect to obtain from a 4D HA CA N HN experiment.[11]

In spite of the reduced dimensionality and the ensuing ease of both data processing and optimizing the experimental parameters, the 3D HA CA N HN experiment has thus been shown to retain the full potentialities of a 4D HA CA N HN data set for identification of all intraresidual backbone connectivities. In principle, if the interresidual two-bond scalar couplings $^2J(^{13}C_i^\alpha,{}^{15}N_{i+1})$ are also included in the derivation of (1), then two pairs of peaks will be expected for each residue i, representing respectively the intraresidual connectivities and the sequential $^{13}C_i^\alpha - {}^{15}N_{i+1}$ connectivities. In a 3D HA CA N HN spectrum, both pairs of peaks would be centered about $\Omega(^{13}C_i^\alpha)$ in the plane belonging to $\Omega(^1H_i^\alpha)$, with the intraresidual connectivity located at $\Omega(^1H_i^N)$ and split by $\Omega(^{15}N_i)$ and the sequential one at $\Omega(^1H_{i+1}^N)$ and split by $\Omega(^{15}N_{i+1})$. However, due to the smaller magnitude of $^2J(^{13}C_i^\alpha,{}^{15}N_{i+1})$ when compared to $^1J(^{13}C_i^\alpha,{}^{15}N_i)$, the sequential connectivities have usually much smaller intensities; in the mixed disulfide of glutaredoxin(C14S) and glutathione, they were observed only for a few residues located in flexible parts of the molecular structure.[19]

Considering that the desired information can also be obtained either by a 4D HA CA N HN experiment or a combination of two 3D triple-resonance experiments, the sensitivity of the 3D HA CA N HN measurement is lower by a factor of $\sqrt{2}$. This results because $\Omega(^{15}N)$ is encoded in the in-phase splitting. However, the fact that peak pairs (rather than single peaks) must be identified in 3D HA CA N HN spectra (Figure 1) greatly facilitates the identification of weak signals, which partly compensates for the intrinsic loss in sensitivity.

When working with smaller molecules, *e.g.*, in protein folding studies with labeled polypeptides or investigations of receptor-bound ligands, similar advantages may result from reducing 3D triple-resonance experiments to two dimensions. It is then recommended to implement the experiments in such a way that $\Omega(^1H^N) \pm \Omega(^{13}C^\alpha)$ is observed along the heteronuclear frequency axis. Since one has for most non-glycyl residues that $\Omega(^{13}C^\alpha) \gg \Omega(^{15}N)$, this results in the appearance of well-separated high-field and low-field regions, which facilitates the spectral analysis. As an illustration, a 2D HN N CA experiment derived from the *ct*-HNNCA scheme of Grzesiek and Bax[20] is presented as supplementary material.

Acknowledgment. Financial support was obtained from the Schweizerischer Nationalfonds (project 31.32033.91) and the Kommission zur Förderung der wissenschaftlichen Forschung (project 2223.1).

Supplementary Material Available: Figure S1, displaying a 2D HN N CA spectrum of the mixed disulphide of *E. coli* gutaredoxin(C14S) with glutathione (2 pages). Ordering information is given on any current masthead page.

(16) Marion, D.; Ikura, K.; Tschudin, R.; Bax, A. *J. Magn. Reson.* **1989**, *85*, 393–399.
(17) Bushweller, J. H.; Aslund, F.; Wüthrich, K.; Holmgren, A. *Biochemistry* **1992**, *31*, 9288–9293.
(18) Bushweller, J. H.; Holmgren, A.; Wüthrich, K. *Eur. J. Biochem.*, submitted for publication.
(19) Bushweller, J. H.; Billeter, M.; Holmgren, A.; Wüthrich, K. *J. Mol. Biol.*, submitted for publication.
(20) Grzesiek, S.; Bax, A. *J. Magn. Reson.* **1992**, *96*, 432–440.
(21) Marion, D.; Ikura, M.; Bax, A. *J. Magn. Reson.* **1989**, *84*, 425–430.
(22) DeMarco, A.; Wüthrich, K. *J. Magn. Reson.* **1976**, *24*, 201–204.
(23) Güntert, P.; Dötsch, V.; Wider, G.; Wüthrich, K. *J. Biomol. NMR* **1992**, *2*, 619–629.
(24) Otting, G.; Wüthrich, K. *J. Magn. Reson.* **1988**, *76*, 569–574.
(25) Shaka, A. J.; Lee, C. J.; Pines, A. *J. Magn. Reson.* **1988**, *77*, 274–293.
(26) Shaka, A. J.; Keeler, J.; Frenkiel, T.; Freeman, R. *J. Magn. Reson.* **1983**, *52*, 335–336.